Dynamic Modeling and Control of a Zeta Converter

E. Vuthchhay[1], C. Bunlaksananusorn[1], and H. Hirata[2]

[1] Faculty of Engineering, King Mongkut's Institute of Technology Ladkrabang (KMITL), Bangkok 10520, Thailand
[2] Department of Applied Computer Engineering, Tokai University, Kanagawa 259-1292, Japan

***Abstract*— A Zeta converter is a fourth-order dc-dc converter made up of two inductors and two capacitors and capable of operating in either step-up or step-down mode. Compared with other converters in the same class, such as Cuk and Sepic converters, the Zeta converter has received the least attention, and more importantly, its dynamic modeling and control have never been reported before in the literature. This paper presents dynamic modeling and control of a Zeta converter. The State-Space Averaging (SSA) technique is applied to find small-signal linear dynamic model of the converter, whereby various transfer functions of the converter can be determined. Based on the control-to-output transfer function, the compensator in PWM feedback loop can be designed to regulate the output voltage. Simulation results show that the converter exhibits good performance during a start-up and step load change.**

I. INTRODUCTION

Nowadays, a dc-dc converter is widely used as a power supply in electronic systems. The converter incorporates feedback control to regulate its output voltage. However, the changes in an input voltage and/or load current will cause the converter's output voltage to deviate from the desired value. It is a task of the feedback control to correct this error and quickly bring the output voltage back into the regulated level. Modeling plays a key role in revealing the insight of the converter's dynamic behavior as well as providing a basis for feedback control design. In the last two decades, there has been a continually active research on dc-dc converters; as a consequence, several modeling methods have been proposed [1]. Among them, State-Space Averaging (SSA) technique [2] is one of the best-known methods. It provides a systematic way to model the converter and has gained widespread acceptance. The SSA modeling technique consists of three stages: (1) Formulation of the state-space equations of the converter for each subinterval in a switching cycle, (2) Average of these equations to get a single averaged state-space equation, and (3) Perturbation of the averaged equation to get a linear small-signal state-space equation, from which various transfer functions of the converter can be determined. Since the SSA is a matrix-based technique, i.e. all the steps above are carried out in a matrix form, formal matrix treatment can be applied to facilitate the modeling process.

The SSA technique was commonly used to model the second-order converters such as buck, boost, and buck-boost converters [2-4]. The modeling of the fourth-order converters such as Cuk and Sepic converters has also been studied [5-7]; however, the used techniques were based on circuit averaging. Like Cuk and Sepic converters, a Zeta converter is the fourth-order converter made up of two inductors and two capacitors and capable of working in either step-up or step-down mode. So far, the dynamic modeling and control of the Zeta converter have never been reported before in the literature. This paper, therefore, presents dynamic modeling and control of a Zeta converter. The SSA technique [2] is applied to find small-signal linear dynamic model of the converter, whereby the various transfer functions of the converter can be determined. Of these, the control-to-output transfer function is used for feedback control design. This transfer function has two pairs of the complex poles on the left half plane and a pair of the complex zeros which can locate either on the left or right half plane, depending on the circuit parameters. The Right-Half-Plane (RHP) zeros are undesirable because they cause extra 360 degrees phase-lag to the control-to-output transfer function. In this paper, the condition to avoid the RHP zeros is established. Finally, based on the control-to-output transfer function, the compensator in PWM feedback loop is designed to regulate an output voltage of the converter.

II. OVERVIEW OF SSA TECHNIQUE

For dc-dc converters operating in Continuous Conduction Mode (CCM), there exist two circuit states within one switching period, T. One is when the MOSFET is turned on for an interval dT, and another is when the MOSFET is turned off for an interval (1-d)T, where d is a duty cycle. The state-space equations for these two circuit states are represented by:

$$\begin{cases} \dfrac{d\mathbf{x}(t)}{dt} = \mathbf{A}_1\mathbf{x}(t) + \mathbf{B}_1\mathbf{u}(t) \\ \mathbf{y}(t) = \mathbf{C}_1\mathbf{x}(t) + \mathbf{E}_1\mathbf{u}(t) \end{cases} \quad (1)$$

$$\begin{cases} \dfrac{d\mathbf{x}(t)}{dt} = \mathbf{A}_2\mathbf{x}(t) + \mathbf{B}_2\mathbf{u}(t) \\ \mathbf{y}(t) = \mathbf{C}_2\mathbf{x}(t) + \mathbf{E}_2\mathbf{u}(t) \end{cases} \quad (2)$$

To find the averaged behavior of the converter over one switching period, (1) and (2) are weighed average by the duty cycle:

$$\begin{cases} \dfrac{d\mathbf{x}(t)}{dt} = \mathbf{A}_S\mathbf{x}(t) + \mathbf{B}_S\mathbf{u}(t) \\ \mathbf{y}(t) = \mathbf{C}_S\mathbf{x}(t) + \mathbf{E}_S\mathbf{u}(t) \end{cases} \quad (3)$$

where

$\mathbf{A}_S = \mathbf{A}_1 d + \mathbf{A}_2(1-d)$, $\mathbf{B}_S = \mathbf{B}_1 d + \mathbf{B}_2(1-d)$, $\mathbf{C}_S = \mathbf{C}_1 d + \mathbf{C}_2(1-d)$, and $\mathbf{E}_S = \mathbf{E}_1 d + \mathbf{E}_2(1-d)$.

Equation (3) is a nonlinear continuous-time equation. It can be linearized by small-signal perturbation with $\mathbf{x} = \mathbf{X} + \tilde{\mathbf{x}}$, $\mathbf{y} = \mathbf{Y} + \tilde{\mathbf{y}}$, $\mathbf{u} = \mathbf{U} + \tilde{\mathbf{u}}$, and $d = D + \tilde{d}$, where the ~ symbol

978-1-4244-2336-1/08/$25.00 © 2008 IEEE

represents a small signal value and the capital letter a dc value. It should be noted that $\mathbf{X} >> \tilde{\mathbf{x}}$, $\mathbf{Y} >> \tilde{\mathbf{y}}$, $\mathbf{U} >> \tilde{\mathbf{u}}$, and $D >> \tilde{d}$. The perturbation yields the steady-state and linear small-signal state-space equations in (4) and (5) respectively.

$$\begin{cases} \dfrac{d\mathbf{X}}{dt} = \mathbf{AX} + \mathbf{BU} = 0 \\ \mathbf{Y} = \mathbf{CX} + \mathbf{EU} \end{cases} \tag{4}$$

$$\begin{cases} \dfrac{d\tilde{\mathbf{x}}(t)}{dt} = \mathbf{A}\tilde{\mathbf{x}}(t) + \mathbf{B}\tilde{\mathbf{u}}(t) + \mathbf{B}_{\mathbf{d}}\tilde{d}(t) \\ \tilde{\mathbf{y}}(t) = \mathbf{C}\tilde{\mathbf{x}}(t) + \mathbf{E}\tilde{\mathbf{u}}(t) + \mathbf{E}_{\mathbf{d}}\tilde{d}(t) \end{cases} \tag{5}$$

where

$\mathbf{A} = \mathbf{A}_1 D + \mathbf{A}_2(1-D)$, $\mathbf{B} = \mathbf{B}_1 D + \mathbf{B}_2(1-D)$, $\mathbf{C} = \mathbf{C}_1 D + \mathbf{C}_2(1-D)$, $\mathbf{E} = \mathbf{E}_1 D + \mathbf{E}_2(1-D)$, $\mathbf{B}_{\mathbf{d}} = (\mathbf{A}_1 - \mathbf{A}_2)\mathbf{X} + (\mathbf{B}_1 - \mathbf{B}_2)\mathbf{U}$, and $\mathbf{E}_{\mathbf{d}} = (\mathbf{C}_1 - \mathbf{C}_2)\mathbf{X} + (\mathbf{E}_1 - \mathbf{E}_2)\mathbf{U}$.

The steady-state solution of the converter can be found by solving (4), which gives:

$$\begin{cases} \mathbf{X} = -\mathbf{A}^{-1}\mathbf{BU} \\ \mathbf{Y} = (-\mathbf{CA}^{-1}\mathbf{B} + \mathbf{E})\mathbf{U} \end{cases} \tag{6}$$

The small-signal transfer function of the converter can be found by applying the Laplace transform to (5). In a matrix form, we get:

$$\begin{cases} \tilde{\mathbf{x}}(s) = \left[(s\mathbf{I} - \mathbf{A})^{-1}\mathbf{B} \quad (s\mathbf{I} - \mathbf{A})^{-1}\mathbf{B}_{\mathbf{d}} \right] \begin{bmatrix} \tilde{\mathbf{u}}(s) \\ \tilde{d}(s) \end{bmatrix} \\ \tilde{\mathbf{y}}(s) = \left[\mathbf{C}(s\mathbf{I} - \mathbf{A})^{-1}\mathbf{B} + \mathbf{E} \quad \mathbf{C}(s\mathbf{I} - \mathbf{A})^{-1}\mathbf{B}_{\mathbf{d}} + \mathbf{E}_{\mathbf{d}} \right] \begin{bmatrix} \tilde{\mathbf{u}}(s) \\ \tilde{d}(s) \end{bmatrix} \end{cases} \tag{7}$$

In the dc-dc converters, the input variable $\tilde{\mathbf{u}}$ usually contains the input voltage and load current. Hence, $\tilde{\mathbf{u}}$ is express as $\tilde{\mathbf{u}}= [u_1\ u_2]^{\mathrm{T}}$, the matrix $\mathbf{B}$ as $\mathbf{B}=[\mathbf{B_{u1}}\ \mathbf{B_{u2}}]$, and the matrix $\mathbf{E}$ as $\mathbf{E}=[\mathbf{E_{u1}}\ \mathbf{E_{u2}}]$. Therefore, (7) becomes:

$$\begin{cases} \tilde{\mathbf{x}}(s) = \left[(s\mathbf{I} - \mathbf{A})^{-1}\mathbf{B}_{\mathrm{u1}} \quad (s\mathbf{I} - \mathbf{A})^{-1}\mathbf{B}_{\mathrm{u2}} \quad (s\mathbf{I} - \mathbf{A})^{-1}\mathbf{B}_{\mathbf{d}} \right] \begin{bmatrix} \tilde{u}_1(s) \\ \tilde{u}_2(s) \\ \tilde{d}(s) \end{bmatrix} \\ \tilde{\mathbf{y}}(s) = \left[\mathbf{C}(s\mathbf{I} - \mathbf{A})^{-1}\mathbf{B}_{\mathrm{u1}} + \mathbf{E}_{\mathrm{u1}} \quad \mathbf{C}(s\mathbf{I} - \mathbf{A})^{-1}\mathbf{B}_{\mathrm{u2}} + \mathbf{E}_{\mathrm{u2}} \quad \mathbf{C}(s\mathbf{I} - \mathbf{A})^{-1}\mathbf{B}_{\mathbf{d}} + \mathbf{E}_{\mathbf{d}} \right] \begin{bmatrix} \tilde{u}_1(s) \\ \tilde{u}_2(s) \\ \tilde{d}(s) \end{bmatrix} \end{cases} \tag{8}$$

For the fourth-order converter, $(s\mathbf{I}–\mathbf{A})^{-1}\mathbf{B_{u1}}$, $(s\mathbf{I}–\mathbf{A})^{-1}\mathbf{B_{u2}}$, and $(s\mathbf{I}–\mathbf{A})^{-1}\mathbf{B_d}$ are the matrices that have four rows and one column. So, (8) can be expanded into:

$$\begin{cases} \tilde{\mathbf{x}}(s) = \begin{bmatrix} G_{vi_1}(s) & G_{zi_1}(s) & G_{di_1}(s) \\ G_{vi_2}(s) & G_{zi_2}(s) & G_{di_2}(s) \\ G_{vv_1}(s) & G_{zv_1}(s) & G_{dv_1}(s) \\ G_{vv_2}(s) & G_{zv_2}(s) & G_{dv_2}(s) \end{bmatrix} \begin{bmatrix} \tilde{u}_1(s) \\ \tilde{u}_2(s) \\ \tilde{d}(s) \end{bmatrix} \\ \tilde{\mathbf{y}}(s) = \begin{bmatrix} G_{vv}(s) & G_{zv}(s) & G_{dv}(s) \end{bmatrix} \begin{bmatrix} \tilde{u}_1(s) \\ \tilde{u}_2(s) \\ \tilde{d}(s) \end{bmatrix} \end{cases} \tag{9}$$

where

$G_{vi_1}(s) = [(s\mathbf{I} - \mathbf{A})^{-1}\mathbf{B}_{\mathrm{u1}}]_{11}$, $G_{zi_1}(s) = [(s\mathbf{I} - \mathbf{A})^{-1}\mathbf{B}_{\mathrm{u2}}]_{11}$, $G_{di_1}(s) = [(s\mathbf{I} - \mathbf{A})^{-1}\mathbf{B}_{\mathbf{d}}]_{11}$,
$G_{vi_2}(s) = [(s\mathbf{I} - \mathbf{A})^{-1}\mathbf{B}_{\mathrm{u1}}]_{21}$, $G_{zi_2}(s) = [(s\mathbf{I} - \mathbf{A})^{-1}\mathbf{B}_{\mathrm{u2}}]_{21}$, $G_{di_2}(s) = [(s\mathbf{I} - \mathbf{A})^{-1}\mathbf{B}_{\mathbf{d}}]_{21}$,
$G_{vv_1}(s) = [(s\mathbf{I} - \mathbf{A})^{-1}\mathbf{B}_{\mathrm{u1}}]_{31}$, $G_{zv_1}(s) = [(s\mathbf{I} - \mathbf{A})^{-1}\mathbf{B}_{\mathrm{u2}}]_{31}$, $G_{dv_1}(s) = [(s\mathbf{I} - \mathbf{A})^{-1}\mathbf{B}_{\mathbf{d}}]_{31}$,
$G_{vv_2}(s) = [(s\mathbf{I} - \mathbf{A})^{-1}\mathbf{B}_{\mathrm{u1}}]_{41}$, $G_{zv_2}(s) = [(s\mathbf{I} - \mathbf{A})^{-1}\mathbf{B}_{\mathrm{u2}}]_{41}$, $G_{dv_2}(s) = [(s\mathbf{I} - \mathbf{A})^{-1}\mathbf{B}_{\mathbf{d}}]_{41}$,
$G_{vv}(s) = \mathbf{C}(s\mathbf{I} - \mathbf{A})^{-1}\mathbf{B}_{\mathrm{u1}} + \mathbf{E}_{\mathrm{u1}}$, $G_{zv}(s) = \mathbf{C}(s\mathbf{I} - \mathbf{A})^{-1}\mathbf{B}_{\mathrm{u2}} + \mathbf{E}_{\mathrm{u2}}$, and
$G_{dv}(s) = \mathbf{C}(s\mathbf{I} - \mathbf{A})^{-1}\mathbf{B}_{\mathbf{d}} + \mathbf{E}_{\mathbf{d}}$

III. Modeling of a Zeta Converter By SSA Technique

A Zeta converter is shown in Fig. 1(a). It is comprised of the MOSFET switch (Q), diode (D), two capacitors (C_1 and C_2), and two inductors (L_1 and L_2). The resistor, R, represents a standing load, and the current source, I_Z, models the load current. The resistors, r_{C1}, r_{C2}, r_{L1}, and r_{L2}, are an equivalent series resistance of the capacitors and inductors respectively. Their values are usually very small, compared to R. In the ideal converter, these equivalent series resistance will be zero.

In CCM, the converter exhibits two circuit states. The first state is when the MOSFET switch is turned on (Fig. 1(b)). During this interval (dT), the inductors L_1 and L_2 are in a charging phase, and hence i_{L1} and i_{L2} increase linearly as shown in Fig. 2. The second state is when the MOSFET switch is turned off (Fig. 1(c)). During this interval ((1-d)T), L_1 and L_2 are in a discharging phase; L_1 discharges the stored energy to C_1, and L_2 discharges the stored energy to output section. Thus, i_{L1} and i_{L2} decrease linearly as shown in Fig. 2.

The output voltage, V_O, is a dc voltage that contains small ripple due to the switching action. For the ideal Zeta converter, the relationship between V_O and V_g is given by:

$$M = \frac{V_o}{V_g} = \frac{D}{1-D} \tag{10}$$

where M is a voltage conversion ratio. It can be seen that V_O could be larger or smaller than V_g, depending on the duty cycle. From Fig. 2., the averaged inductor currents, I_{L1} and I_{L2}, must be greater than one-half of their ripple components, Δi_{L1} and Δi_{L2}, for the circuit to remain in CCM [8]. It can be shown that for CCM operation L_1 and L_2 must satisfy the following conditions:

$$\begin{cases} L_1 > \dfrac{(1-D)^2 R}{2Df}\left(1 + \dfrac{r_{L2}}{R} + \dfrac{r_{C1}}{R}\dfrac{D}{1-D}\right) \\ L_2 > \dfrac{(1-D)R}{2f}\left(1 + \dfrac{r_{L2}}{R}\right) \end{cases} \tag{11}$$

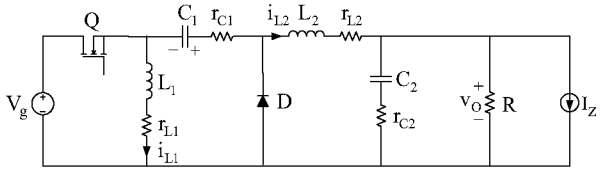

(a) Zeta converter.

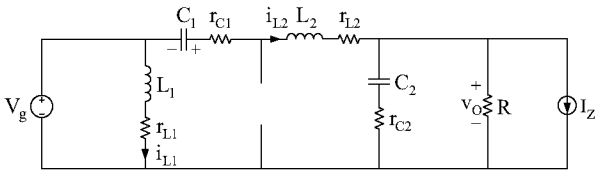

(b) Zeta converter when MOSFET is turned on.

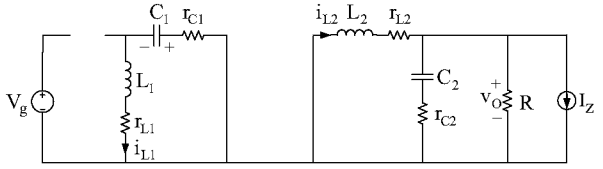

(c) Zeta converter when MOSFET is turned off.

Fig. 1. Operation of Zeta converter.

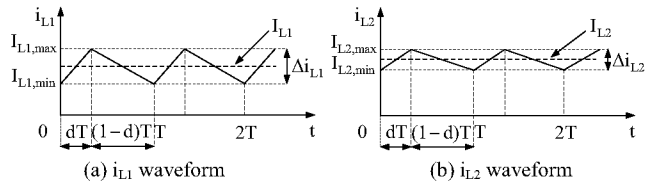

(a) i_{L1} waveform (b) i_{L2} waveform

Fig. 2. Current waveforms.

A. State-Space Description

The state-space equations of the Zeta converter for the on and off states of the switch can be written from Fig. 1(b) and (c) respectively, which is given in (12):

$$\begin{aligned}
\frac{di_{L1}}{dt} &= \frac{r_{C1}}{L_1}(\delta-1)i_{L1} - \frac{r_{L1}}{L_1} + \frac{v_{C1}}{L_1}(\delta-1) + \frac{V_g}{L_1}\delta \\
\frac{di_{L2}}{dt} &= \frac{-1}{L_2}(r_{L2}+r_{C1}\delta + \frac{r_{C2}R}{r_{C2}+R})i_{L2} + \frac{v_{C1}}{L_2}\delta - \frac{R}{L_2(r_{C2}+R)}v_{C2} + \frac{V_g}{L_2}\delta + \frac{r_{C2}R}{L_2(r_{C2}+R)}I_Z \\
\frac{dv_{C1}}{dt} &= \frac{i_{L1}}{C_1}(1-\delta) - \frac{i_{L2}}{C_1}\delta \\
\frac{dv_{C2}}{dt} &= \frac{R}{C_2(r_{C2}+R)}i_{L2} - \frac{1}{C_2(r_{C2}+R)}v_{C2} - \frac{R}{C_2(r_{C2}+R)}I_Z \\
v_O &= \frac{r_{C2}R}{r_{C2}+R}i_{L2} + \frac{R}{r_{C2}+R}v_{C2} - \frac{r_{C2}R}{r_{C2}+R}I_Z
\end{aligned} \tag{12}$$

Note that the equations are expressed in a compact form using the switching function, δ. When the switch is on, δ =1, (12) will become the on-state equation. When the switch is off, δ =0, (12) will become the off-state equation.

The averaged matrices for the steady-state and the linear small-signal state-space equations can be written according to (4) and (5).

$$\mathbf{A} = \begin{bmatrix} -\frac{r_{C1}(1-D)+r_{L1}}{L_1} & 0 & -\frac{1-D}{L_1} & 0 \\ 0 & -\frac{(r_{C2}+R)(Dr_{C1}+r_{L2})+r_{C2}R}{L_2(r_{C2}+R)} & \frac{D}{L_2} & \frac{-R}{L_2(r_{C2}+R)} \\ \frac{1-D}{C_1} & \frac{-D}{C_1} & 0 & 0 \\ 0 & \frac{R}{C_2(r_{C2}+R)} & 0 & \frac{-1}{C_2(r_{C2}+R)} \end{bmatrix} \tag{13}$$

$$\mathbf{B} = \begin{bmatrix} \frac{D}{L_1} & 0 \\ \frac{D}{L_2} & \frac{r_{C2}R}{L_2(r_{C2}+R)} \\ 0 & 0 \\ 0 & \frac{-R}{C_2(r_{C2}+R)} \end{bmatrix} \tag{14}$$

$$\mathbf{C} = \begin{bmatrix} 0 & \frac{r_{C2}R}{r_{C2}+R} & 0 & \frac{r_{C2}R}{r_{C2}+R} \end{bmatrix} \tag{15}$$

$$\mathbf{E} = \begin{bmatrix} 0 & \frac{-r_{C2}R}{r_{C2}+R} \end{bmatrix} \tag{16}$$

$$\mathbf{B_d} = \frac{\eta}{R(1-D)^2}\begin{bmatrix} \frac{1}{L_1}[V_g[(1-D)(R+r_{L2})+Dr_{C1}]-I_Z Dr_{L1}R] \\ \frac{1}{L_2}[V_g(r_{L2}+R)(1-D)-[r_{C1}(1-D)+Dr_{L1}]RI_Z] \\ \frac{-1}{C_1}[DV_g+RI_Z(1-D)] \\ 0 \end{bmatrix} \tag{17}$$

$$\mathbf{E_d} = [0] \tag{18}$$

B. Steady-State Equations

Given the averaged matrices from (13) to (18), the steady-state solution of the converter can be obtained from (6):

$$\begin{cases} \begin{bmatrix} I_{L1} \\ I_{L2} \\ V_{C1} \\ V_{C2} \end{bmatrix} = M\eta \begin{bmatrix} \frac{D}{R(1-D)} & 1 \\ \frac{1}{R} & \frac{1}{M} \\ 1+\frac{r_{L2}}{R}-\frac{r_{L1}}{R}M & -(r_{C1}+r_{L1}\frac{1}{1-D}) \\ 1 & -(r_{C1}+r_{L1}M+r_{L2}\frac{1}{M}) \end{bmatrix} \begin{bmatrix} V_g \\ I_Z \end{bmatrix} \\ V_O = [V_g - I_Z(r_{C1}+r_{L1}M+r_{L2}\frac{1}{M})]M\eta \end{cases} \tag{19}$$

where $\eta = \dfrac{1}{1+\frac{r_{L2}}{R}+\frac{r_{C1}}{R}M+\frac{r_{L1}}{R}M^2}$ and $M = \dfrac{D}{1-D}$.

Notice that if r_{C1}, r_{C2}, r_{L1}, and r_{L2} are assumed to be zero, the output equation in (19) will be reduced to $M=V_O/V_g=D/(1-D)$, the same as the expression for the ideal converter in (10).

C. Linear Small-Signal State-Space Equations

Given the averaged matrices (13) to (18), the linear small-signal state-space equations of the Zeta converter can be formulated in according with (5):

$$\begin{aligned} \frac{d}{dt}\begin{bmatrix} \tilde{i}_{L1}(t) \\ \tilde{i}_{L2}(t) \\ \tilde{v}_{C1}(t) \\ \tilde{v}_{C2}(t) \end{bmatrix} &= \begin{bmatrix} \frac{r_{C1}(1-D)+r_{L1}}{L_1} & 0 & -\frac{1-D}{L_1} & 0 \\ 0 & -\frac{(r_{C2}+R)(Dr_{C1}+r_{L2})+r_{C2}R}{L_2(r_{C2}+R)} & \frac{D}{L_2} & \frac{-R}{L_2(r_{C2}+R)} \\ \frac{1-D}{C_1} & -\frac{D}{C_1} & 0 & 0 \\ 0 & \frac{R}{C_2(r_{C2}+R)} & 0 & \frac{-1}{C_2(r_{C2}+R)} \end{bmatrix}\begin{bmatrix} \tilde{i}_{L1}(t) \\ \tilde{i}_{L2}(t) \\ \tilde{v}_{C1}(t) \\ \tilde{v}_{C2}(t) \end{bmatrix} + \\ &\quad \begin{bmatrix} \frac{D}{L_1} & 0 & \frac{\eta[V_g[(1-D)(R+r_{L2})+Dr_{C1}]-I_Z Dr_{L1}R]}{L_1R(1-D)^2} \\ \frac{D}{L_2} & \frac{r_{C2}R}{L_2(r_{C2}+R)} & \frac{\eta[V_g(r_{L2}+R)(1-D)-I_ZR[r_{C1}(1-D)+Dr_{L1}]]}{L_2R(1-D)^2} \\ 0 & 0 & \frac{-\eta[DV_g+RI_Z(1-D)]}{C_1R(1-D)^2} \\ 0 & -\frac{R}{C_2(r_{C2}+R)} & 0 \end{bmatrix}\begin{bmatrix} \tilde{v}_g(t) \\ \tilde{i}_Z(t) \\ \tilde{d}(t) \end{bmatrix} \end{aligned} \tag{20}$$

$$\tilde{v}_O(t) = \begin{bmatrix} 0 & \frac{r_{C2}R}{r_{C2}+R} & 0 & \frac{r_{C2}R}{r_{C2}+R} \end{bmatrix}\begin{bmatrix} \tilde{i}_{L1}(t) \\ \tilde{i}_{L2}(t) \\ \tilde{v}_{C1}(t) \\ \tilde{v}_{C2}(t) \end{bmatrix} + \begin{bmatrix} 0 & \frac{-r_{C2}R}{r_{C2}+R} & 0 \end{bmatrix}\begin{bmatrix} \tilde{v}_g(t) \\ \tilde{i}_Z(t) \\ \tilde{d}(t) \end{bmatrix}$$

D. Finding Transfer Functions

Referring to (9), fifteen transfer functions can be determined from (20). However, only a few of them are useful for feedback control design. These transfer functions are:

The duty ratio-to-output voltage transfer function

$$\begin{aligned} G_{dv}(s) &= \frac{\tilde{v}_O(s)}{\tilde{d}(s)} = \mathbf{C(sI-A)^{-1}B_d + E_d} \\ &= \frac{\eta}{(1-D)^2}\frac{(a_{dv}s^2+b_{dv}s+c_{dv})(d_{dv}s+1)}{as^4+bs^3+cs^2+ds+e} \end{aligned} \tag{21}$$

The input voltage-to-output voltage transfer function

$$\begin{aligned} G_{vv}(s) &= \frac{\tilde{v}_O(s)}{\tilde{v}_g(s)} = \mathbf{C(sI-A)^{-1}B_{u1} + E_{u1}} \\ &= DR\frac{(a_{vv}s^2+b_{vv}s+c_{vv})(d_{vv}s+1)}{as^4+bs^3+cs^2+ds+e} \end{aligned} \tag{22}$$

The output impedance transfer function

$$\begin{aligned} G_{zv}(s) &= \frac{\tilde{v}_O(s)}{\tilde{i}_Z(s)} = \mathbf{C(sI-A)^{-1}B_{u2} + E_{u2}} \\ &= -R\frac{(a_{zv}s^2+b_{zv}s+c_{zv})(d_{zv}s+1)}{as^4+bs^3+cs^2+ds+e} \end{aligned} \tag{23}$$

The coefficients in (21) to (23) are listed in TABLE I.

TABLE I
COEFFICIENTS OF $G_{dv}(s)$, $G_{zv}(s)$, AND $G_{vv}(s)$.

$a_{dv}=L_1C_1[V_g(1-D)(R+r_{L2})-I_ZR[(1-D)r_{C1}+Dr_{L1}]$, $b_{dv}=-V_g[L_1D^2-C_1(1-D)(R+r_{L2})[(1-D)r_{C1}+r_{L1}]]$ $-I_ZR[L_1D(1-D)+r_{C1}^2C_1(1-D)^2+r_{L1}C_1(r_{C1}+r_{L1}D-D^2r_{C1})]$, $c_{dv}=V_g[(1-D)^2(R+r_{L2})-D^2r_{L1}]-I_ZR(1-D)[2Dr_{L1}+r_{C1}(1-D)]$, $d_{dv}=C_2r_{C2}$.
$a_{vv}=C_1L_1$, $b_{vv}=C_1[r_{L1}+r_{C1}(1-D)]$, $c_{vv}=1-D$, $d_{vv}=C_2r_{C2}$.
$a_{zv}=L_1L_2C_1C_2r_{C2}$, $e_{zv}=r_{C1}D(1-D)+r_{L1}D^2+r_{L2}(1-D)^2$, $b_{zv}=L_1C_1(L_2+Dr_{C2}r_{C1}C_2)+(1-D)r_{C1}r_{C2}L_2C_1C_2+(L_1r_{L2}+L_2r_{L1})r_{C2}C_1C_2$, $c_{zv}=(1-D)[(1-D)r_{C2}L_2C_2+r_{C1}C_1(L_2+Dr_{C1}r_{C2}C_2+r_{C2}r_{L2}C_2)]+L_1D(Dr_{C2}C_2+r_{C1}C_1)$ $+C_1[r_{L1}r_{C2}C_2(r_{C1}D+r_{L2})+r_{L1}L_2+r_{L2}L_1]$, $d_{zv}=L_1D^2+(1-D)[(1-D)(L_2+r_{C2}r_{L2}C_2)+Dr_{C1}(r_{C1}C_1+r_{C2}C_2)+r_{C1}r_{L2}C_1]$ $+r_{L1}(C_1r_{L2}+C_1Dr_{C1}+r_{C2}D^2C_2)$.
$a=L_1C_1L_2C_2(R+r_{C2})$, $e=(1-D)^2(R+r_{L2})+r_{C1}D(1-D)+r_{L1}D^2$, $b=L_1C_1(L_2+r_{C2}C_2R)+C_1(R+r_{C2})[r_{C1}L_2C_2(1-D)+Dr_{C1}L_1C_2+C_2(r_{L2}L_1+r_{L1}L_2)]$ $c=(1-D)[[(1-D)L_2+(Dr_{C1}+r_{L2})r_{C1}C_1](r_{C2}+R)C_2+r_{C1}C_1(r_{C2}C_2R+L_2)]$ $+C_2(r_{C2}+R)[L_1D^2+(Dr_{C1}+r_{L2})r_{L1}C_1]+C_1[L_1(Dr_{C1}+R)+r_{L1}L_2+r_{L2}L_1+r_{L1}r_{C2}C_2R]$, $d=L_1D^2+(1-D)^2[L_2+r_{C2}C_2R+r_{L2}C_2(R+r_{C2})]+[r_{C1}(1-D)+r_{L1}D](R+r_{C2})DC_2$ $+[(1-D)r_{C1}+r_{L1}](r_{L2}+Dr_{C1}+R)C_1$.

IV. PWM FEEDBACK CONTROL

A. Description of PWM Feedback Control

Fig. 3 (a) shows feedback control of a Zeta converter with PWM technique. The output voltage, v_O, is fed back and compared with the reference voltage, V_{ref}. The resulting error voltage is processed by a controller, $G_C(s)$, which produces the control voltage, v_C, to compare with the sawtooth voltage, v_{saw}, at the PWM comparator. As shown in Fig. 3 (b), the MOSFET is turned on when v_C is larger than v_{saw}, and turned off when v_C is smaller than v_{saw}. If v_O is changed, feedback control will respond by adjusting v_C and the duty cycle of the MOSFET until v_O is again equal to V_{ref}.

Fig. 4 shows a small-signal block diagram of the converter in Fig. 3 (a) The power stage is represented by the three transfer functions: $G_{dv}(s)$, $G_{vv}(s)$, and $G_{zv}(s)$ derived earlier. The transfer function of the PWM comparator can be derived from the waveform in Fig. 3 (b). It is given by:

$$F_M=\frac{\tilde{d}(s)}{\tilde{v}_C(s)}=\frac{1}{V_M} \tag{24}$$

where V_M is an amplitude of the sawtooth voltage. $G_C(s)$ is a controller or compensator. From Fig. 4, the open loop transfer function is defined as:

$$T(s)=G_C(s)G_{dv}(s)F_M \tag{25}$$

Given $G_{dv}(s)$ in (21) and F_M in (24), we can design the compensator $G_C(s)$ by appropriately selecting its poles and zeros so that (25) has high dc gain and reasonable crossover frequency, while possessing sufficient amount of phase margin [1].

Before proceeding to design the compensator, it is worthwhile to firstly examine the transfer function $G_{dv}(s)$ in (21), which has three zeros and four poles. It can be proved by the Routh-Hurwitz criterion [9] that all the poles of $G_{dv}(s)$ are located on the left half plane. The $d_{dv}s+1$ term on the numerator always gives the Left-Half-Plane (LHP) zero since d_{dv} is positive. However, there is a possibility that the quadratic term, $a_{dv}s^2+b_{dv}s+c_{dv}$ can yield a pair of Right-Half-Plane (RHP) zeros. The RHP zeros are undesirable because they contribute additional 360 degrees phase-lag to $G_{dv}(s)$, making feedback loop compensation very difficult. The LHP zeros from the quadratic term are given by:

$$s_{Z1,2}=\frac{-b_{dv}\pm\sqrt{b_{dv}^2-4a_{dv}c_{dv}}}{2a_{dv}}<0 \tag{26}$$

It can be proved that (26) yields only a complex conjugate, not real number. Hence, to avoid the RHP zeros, the following conditions must be satisfied:

$$\begin{cases} b_{dv}^2<4a_{dv}c_{dv} \\ b_{dv}>0 \end{cases} \tag{27}$$

where

$a_{dv}=L_1C_1V_g(1-D)(R+r_{L2})$, $c_{dv}=V_g[(1-D)^2(R+r_{L2})-D^2r_{L1}]$,

and $b_{dv}=-V_g[L_1D^2-C_1(1-D)(R+r_{L2})[(1-D)r_{C1}+r_{L1}]]$.

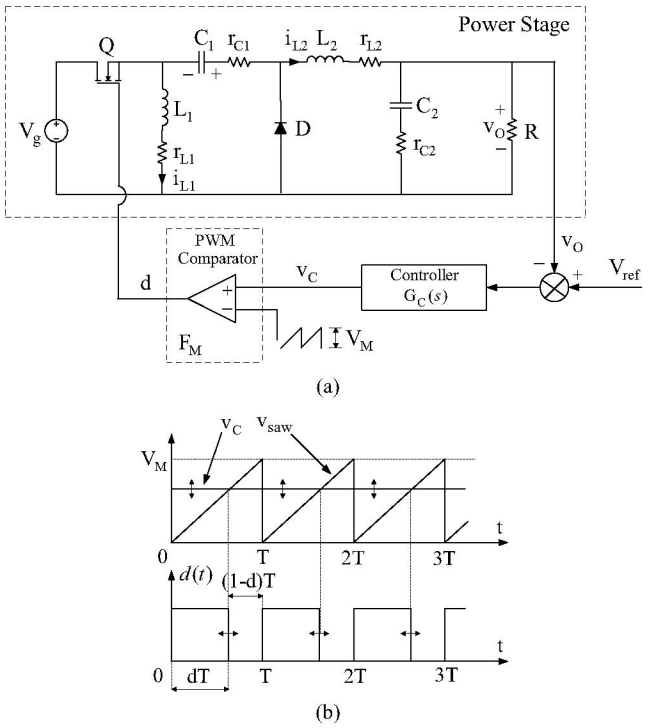

Fig. 3 (a) Zeta converter with PWM feedback control
(b) Waveforms of PWM comparator.

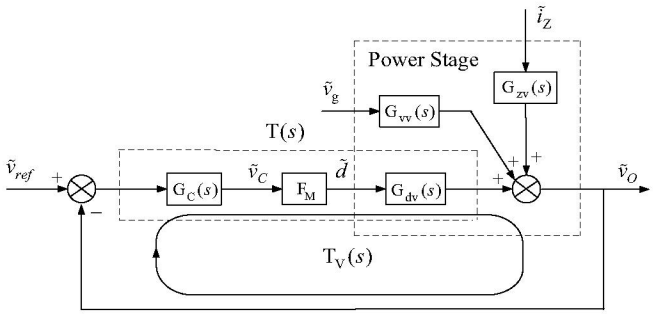

Fig. 4. Small-signal block diagram of Zeta converter with PWM feedback control.

B. *Feedback Loop Compensation*

The compensator design is illustrated with the Zeta converter whose circuit parameters are as shown in Table II. It should be noted that these parameters satisfy both the condition for CCM in (11) and the condition for LHP zeros in (27). Since both the input voltage and load current can vary, the design is performed for the worst case condition, which occurs when Vg = 15V and R = 1Ω. Substituting the relevant parameters from TABLE II into (21) and (24), the product $T_U(s)=F_M G_{dv}(s)$ can be found:

$$T_U(s)=\frac{1.648\text{x}10^4 s^3+8.774\text{x}10^8 s^2+1.758\text{x}10^{12}s+6.505\text{x}10^{16}}{s^4+8452s^3+1.647\text{x}10^8 s^2+5.878\text{x}10^{11}s+4.969\text{x}10^{15}} \quad (28)$$

A PI compensator shown in Fig. 5 has been selected to compensate $T_U(s)$ in (29). Its transfer function is given by:

$$G_C(s)=\frac{z_2}{z_1}=\frac{\omega_O}{s}\left(\frac{s}{\omega_Z}+1\right) \quad (29)$$

where $\omega_O=\frac{1}{R_1C_1}$ and $\omega_Z=\frac{1}{R_2C_1}$.

The pole at the origin helps increase the low frequency gain of the open-loop transfer function, T(s). The zero, ω_Z, and gain, ω_O, can be tuned to give T(s) the desirable crossover frequency and phase margin respectively.

The design objective here is to achieve T(s) with the crossover frequency of 10kHz and phase margin of more than 45 degrees. To achieve this, the zero of $G_C(s)$ has been set at $\omega_Z=3\text{x}10^3$rad/s and the gain at $\omega_O=8.65\text{x}10^3$ rad/s. Based on these values, PI compensator's component values are calculated, getting: R_1=15KΩ, R_2=43KΩ, and C_1=4.7nF. Substitution of the component values into (30) gives:

$$G_C(s)=\frac{8.65\text{x}10^3}{s}\left(\frac{s}{3\text{x}10^3}+1\right) \quad (30)$$

Fig. 6 shows the bode plots of $G_C(s)$ (dotted line), $T_U(s)$ (dashed line), and T(s) (solid line). It can be seen that T(s) has the phase margin of 53 degrees and crossover frequency of 10KHz, meeting the design objective.

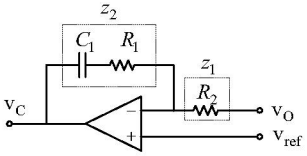

Fig. 5. PI compensator.

TABLE II
CONVERTER PARAMETERS.

Circuit Parameters	Values
V_g	15-20V
V_O	5V
R	1-5Ω
C_1	100μF
C_2	200μF
r_{C1}	0.19Ω
r_{C2}	0.095Ω
L_1	100μH
L_2	55μH
r_{L1}	1mΩ
r_{L2}	0.55mΩ
I_Z	0
V_M	1.8V
T=1/f	10μs

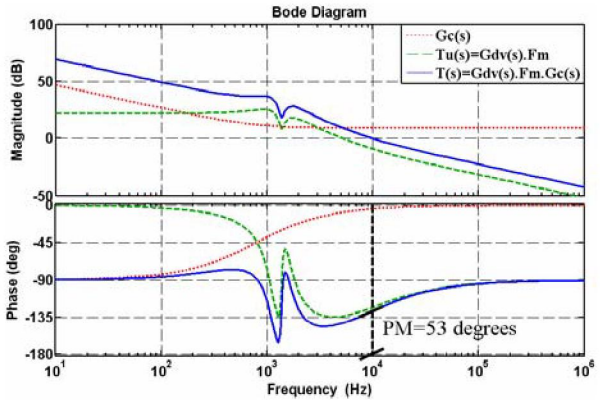

Fig. 6. Bode Plots of $G_C(s)$, $T_U(s)$, and T(s).

V. RESULTS

A SIMULINK model of a PWM controlled Zeta converter is depicted in Fig. 7. The linear small-signal state-space equations in (20), F_M in (24), and $G_C(s)$ in (30) are inputted into the power stage, PWM comparator, and compensator blocks respectively. The mux block combines three input signals (V_g, I_Z, and d) into vector form for using in the power stage block.

Fig. 8 shows the simulated output voltage start-up transient. The output voltage settles to 5V after about 160μs, with the maximum voltage overshoot of 6.3V. Fig. 9 shows the simulated output voltage response, when the load current is switched back and forth between 1A and 3A. The maximum voltage drop/raise during the transient is around 0.28V. The feedback control is able to keep the output voltage at 5V after the transient which lasts about 100μs.

VI. CONCLUSION

In this paper, dynamic modeling and control of a Zeta converter have been presented. The State-Space Averaging (SSA) technique was applied to find the small-signal linear dynamic model of the converter (equation (20)), from which the transfer functions $G_{dv}(s)$ in (21), $G_{vv}(s)$ in (22), and $G_{zv}(s)$ in (23) were derived. $G_{dv}(s)$ was particularly important for feedback control design. The quadratic term on the numerator of $G_{dv}(s)$ could yield the RHP zeros and; to prevent this, the condition in (27) was establish. Based on $G_{dv}(s)$, the compensator in PWM feedback loop was designed to regulate the output voltage. Simulation results show that the converter exhibited good performance during a start-up and step load change.

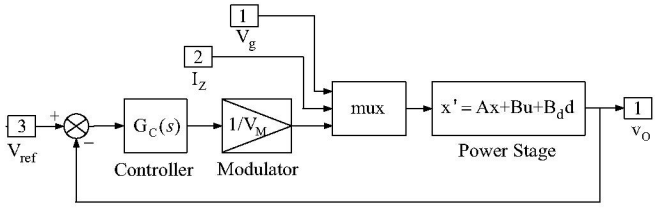

Fig. 7. SIMULINK model of Zeta converter with PWM feedback control.

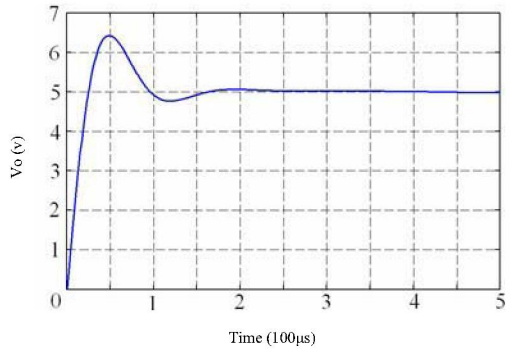

Fig. 8. Output voltage response during a start-up.

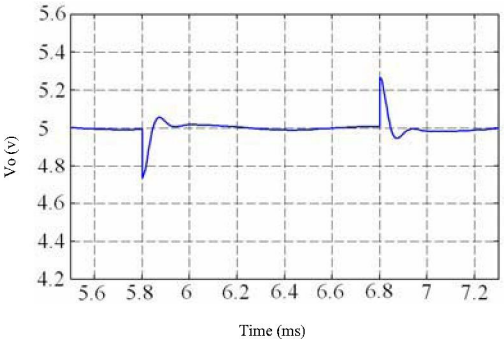

Fig. 9. Output voltage response during the load current back and forth between 1A and 3A.

REFERENCES

[1] R. W. Erickson and D. Maksimović, *Fundamentals of Power Electronics*, 2nd ed., Kluwer Academic Publishers, 2001.

[2] R. D. Middlebook and S. Cuk, "A General Unified Approach to Modeling Switching-Converter Power Stages," *International Journal of Electronics*, vol. 42, pp. 521-550, June 1977.

[3] N. Mohan, T. M. Undeland, and W. P. Robbins, *Power Electronics, Converter, Applications, and Design*, 3rd ed., John Wiley and Sons Inc, 2003.

[4] M. H. Rashid, *Power Electronics Handbook: Devices, Circuits, and Applications*, 2nd ed., Elsevier Inc, 2007.

[5] V. Vorpérian, "The Effect of the Magnetizing Inductance on the Small-Signal Dynamics of the Isolated Cuk Converter," *IEEE trans. on aerospace and electronic systems*, July 1996.

[6] R. Ridley, "Analyzing the Sepic Converter," *Power Systems Design Europe Magazine*, pp. 14-18, November 2006.

[7] A. Hren and P. Slibar, "Full Order Dynamic Model of SEPIC Converter," *Proc. of the IEEE International Symposium on Industrial Electronics*, pp. 553-558, June 2005.

[8] D. W. Hart, *Introduction to Power Electronics*, Prentice Hall Inc, 1997.

[9] B. C. Kuo, *Automatic Control Systems*, 7rd ed., Prentice Hall Inc, 1995.